Semi-confined compression of microfabricated polymerized biomaterial constructs

2011 J. Micromech. Microeng. 21 054014

(http://iopscience.iop.org/0960-1317/21/5/054014)

J. Micromech. Microeng. **21** (2011) 054014 (10pp) doi:10.1088/0960-1317/21/5/054014

Semi-confined compression of microfabricated polymerized biomaterial constructs

Christopher Moraes[1,2], Ruogang Zhao[2], Morakot Likhitpanichkul[1], Craig A Simmons[1,2,3] and Yu Sun[1,2,3]

[1] Department of Mechanical and Industrial Engineering, University of Toronto, 5 King's College Road, Toronto, Ontario, M5S 3G8, Canada
[2] Institute of Biomaterials and Biomedical Engineering, University of Toronto, 164 College Street, Toronto, Ontario, M5S 3G9, Canada

E-mail: sun@mie.utoronto.ca and simmons@mie.utoronto.ca

Received 1 November 2010, in final form 3 February 2011
Published 28 April 2011
Online at stacks.iop.org/JMM/21/054014

Abstract
Mechanical forces are critical parameters in engineering functional tissue because of their established influence on cellular behaviour. However, identifying ideal combinations of mechanical, biomaterial and chemical stimuli to obtain a desired cellular response requires high-throughput screening technologies, which may be realized through microfabricated systems. This paper reports on the development and characterization of a MEMS device for *semi-confined* biomaterial compression. An array of these devices would enable studies involving mechanical deformation of three-dimensional biomaterials, an important parameter in creating physiologically relevant microenvironments *in vitro*. The described device has the ability to simultaneously apply a range of compressive mechanical stimuli to multiple polymerized hydrogel microconstructs. Local micromechanical strains generated within the semi-confined hydrogel cylinders are characterized and compared with those produced in current micro- and macroscale technologies. In contrast to previous work generating unconfined compression in microfabricated devices, the semi-confined compression model used in this work generates uniform regions of strain within the central portion of each hydrogel, demonstrated here to range from 20% to 45% across the array. The uniform strains achieved simplify experimental analysis and improve the utility of the compression platform. Furthermore, the system is compatible with a wide variety of polymerizable biomaterials, enhancing device versatility and usability in tissue engineering and fundamental cell biology studies.

(Some figures in this article are in colour only in the electronic version)

1. Introduction

Mechanical stimulation plays a critical role in regulating cell function [1], modulating or even supplanting cellular response to other physical and biochemical factors in the cellular microenvironment [2, 3]. As such, mechanical forces can be important parameters in controlling cellular function for biomedical applications, such as tissue engineering or regenerative medicine [4]. Bioreactors developed for these purposes often apply mechanical stimuli to cells in a three-dimensional biomaterial matrix, to encourage the formation of functional replacement tissue [5–8].

However, selecting the appropriate mechanical and biochemical stimuli for these studies is largely based on educated guesses. Cellular behaviour is difficult to predict *a priori* because the combined influence of multiple factors on cell function is often nonlinear [9–11], requiring systematic studies of each combination of culture conditions, before designing a bioreactor system [12]. The inclusion of additional

[3] Authors to whom any correspondence should be addressed.

screening parameters exponentially increases the number of experimental conditions to be evaluated and is hence impractical without the use of high-throughput cell culture screening technologies.

Microfabricated systems have been recently developed to address this issue by increasing experimental throughput in screening for the effects of multiple dynamic mechanical stimulation parameters in two-dimensional (2D) *in vitro* culture [13–18]. The importance of encapsulating cells in a physiologically relevant three-dimensional (3D) environment [19], and the influence of mechanical compression on critical cell functions [20–22], prompted our recent work in developing a microfabricated platform to apply a range of dynamic mechanical compression to three-dimensional, cell-laden, biomaterial microconstructs [23]. This platform consisted of an array of cylindrical hydrogel microconstructs photopolymerized over vertically actuated PDMS microposts. A range of compressive strains (6–26%) was simultaneously applied to the unconfined cylindrical constructs across the array, enabling screening of multiple mechanical conditions on a single chip.

Two critical issues limit the utility of our first generation 3D compression-based screening platform: (1) biomaterial compatibility and (2) strain uniformity. First, this platform required a photopolymerizable biomaterial to be micropatterned onto the device array. Limiting studies to photopolymerizable polymers requires thorough lithography optimization studies and, more importantly, excludes many non-photopolymerizable candidate biomaterials, a critical variable in successful tissue engineering [24]. Second, this mode of unconfined compression generates heterogeneous strains in a microconstruct. These non-uniform strain distributions can confound biological analysis and make it difficult to infer the specific stimulation parameters responsible for a biological effect. Thus, although the previous compression platform was useful for certain studies, these issues hinder the broader utility of the microdevice.

Here we report on the development of a microfabricated biomaterial compression device which addresses these concerns of biomaterial limitation and strain heterogeneity. This study focuses on device development, biomaterial integration, and characterization of deformation in a polyethylene glycol hydrogel. For experimental simplicity, no cells were encapsulated in the biomaterials, as this has been previously demonstrated [23]. A semi-confined compression scheme was adopted, and strains generated in microfabricated hydrogel constructs were experimentally determined and quantified using finite element analysis (FEA). The results demonstrate significant improvements in versatility and applicability of this new MEMS-based screening platform over current technologies, criteria that will be of importance in using this technology to both address fundamental questions in cell biology and select rational design strategies for tissue engineering and regenerative medicine.

2. Methods

Unless otherwise stated, all chemicals and reagents for microdevice fabrication and biomaterial handling were purchased from Sigma-Aldrich (Oakville, ON, Canada), and all other equipment and materials from Fisher Scientific (Ottawa, ON, Canada).

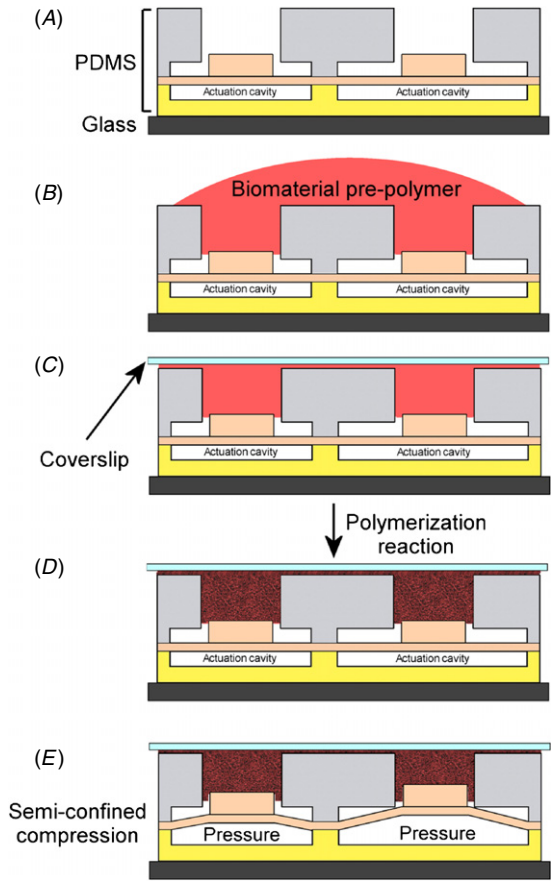

Figure 1. Device schematic. (*A*) Multilayer PDMS device for semi-confined compression of polymerized biomaterial with increased throughput over currently available technologies. (*B*) Biomaterial hydrogel pre-polymer is dispensed over the compression chambers. Surface tension of the liquid prevents flow past the loading piston. (*C*) A glass coverslip is placed over the device, and (*D*) the polymerization reaction is completed. (*E*) Pneumatic pressure actuates the loading piston, compressing the hydrogel. Variation in size of actuation cavity diameter creates a range of compressive strains for a single applied pressure.

2.1. Device overview

The microfabricated semi-confined compression array consists of a multilayered PDMS structure (figure 1(*A*)), in which cylindrical loading pistons are suspended over an actuation cavity. Pneumatic pressure applied to the cavity causes the pistons to displace vertically. As previously demonstrated, modulating the size of the actuation cavity enables a range of vertical actuation heights to be achieved, using a single pressure source [25]. A third PDMS layer confines the liquid biomaterial pre-polymer to the cylindrical region above the loading piston. Surface tension of the pre-polymer prevents liquid flow into the microdevice (figure 1(*B*)). The biomaterial is polymerized *in situ* beneath a glass coverslip (figures 1(*C*) and (*D*)), and compressive strains are then applied by pneumatically raising the loading pistons (figure 1(*E*)).

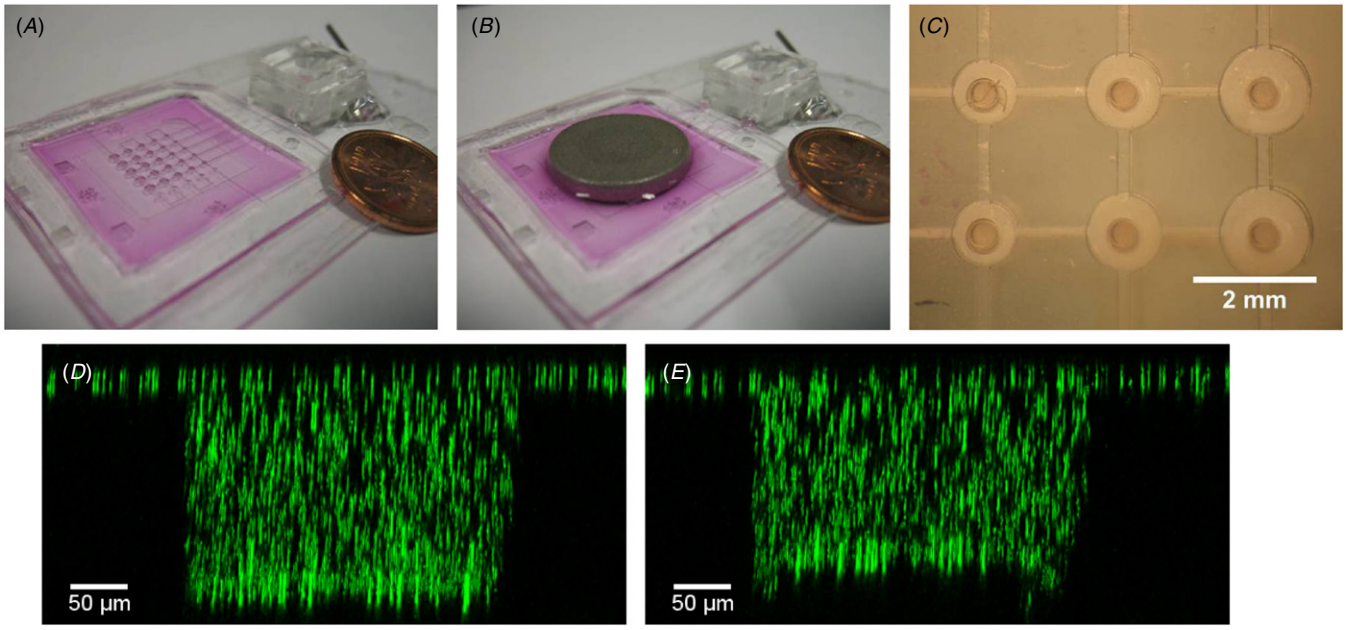

Figure 2. Device operation. (*A*) 5 × 5 array of semi-confined compression chambers under a coverslip. Larger device arrays have been previously demonstrated using a similar fabrication technique [25]. (*B*) The coverslip is replaced by a porous sintered disc to allow fluid flow during mechanical compression. (*C*) Collagen hydrogel polymerized *in situ*. (*D*) and (*E*) Confocal microscopy images are resliced to obtain a side view of fluorescent markers polymerized in the hydrogel at (*D*) rest and (*E*) under compression.

2.2. Device fabrication

Briefly, single and multi-layer SU-8 masters were fabricated on glass microscope slides, as per the manufacturer's instructions. Exclusion moulding was used to create patterned PDMS replica films [26], which were then aligned and bonded on a 3″ × 2″ glass slide to create a multilayer stack. This method eliminates shrinkage-induced alignment registration errors, a common problem in building arrayed multilayer PDMS devices at this scale [25]. For these experiments, loading pistons were fabricated to be 400 μm in diameter and were supported on an 80 μm thick PDMS film suspended over an actuation cavity. Loading pistons were designed to have an ∼100 μm range of unimpeded vertical motion into the compression chambers. A variety of vertical displacements were obtained simultaneously across the array by using a single pressure source and varying actuation cavity diameters. In these experiments 0 (control), 800, 1000, 1200 and 1400 μm diameter actuation cavities were fabricated beneath the loading pistons. Compression chambers containing the polymerized biomaterials were designed to be 500 μm in diameter and 200 μm in thickness. With a 2.25 mm pitch, 25 compression chambers were arrayed in a 5 × 5 array within a 2 cm^2 area. The ability to use this fabrication process to produce larger arrays has been previously demonstrated [25]. A PDMS connector was bonded to the pneumatic pressure channel, and a PDMS gasket was positioned to hold the liquid biomaterial prepolymer (figure 2(*A*)).

Devices were sterilized by soaking in 70% ethanol for 5 min, followed by air-drying in a biosafety cabinet, and exposure to germicidal UV light for 30 min. When ready for actuation, devices were connected to off-chip peripheral pneumatic equipment. Pneumatic pressures of 55 kPa are generated using an eccentric diaphragm pump (SP 500 EC-LC; Schwarzer Precision; Germany). A solenoid valve (Pneumadyne; Plymouth, MN, USA) was used to apply and vent pressure to the microdevice.

2.3. Hydrogel preparation

Polyethylene glycol (PEG) hydrogels were polymerized by photochemistry. A hydrogel precursor solution of 10% w/v polyethylene glycol diacrylate (PEGDA; 3.4 kDa, Laysan Bio; Arab, AL, USA) and 10% w/v PEG (8 kDa, Sigma) was prepared in Dulbecco's Medium Eagle Media (DMEM). A photoinitiator stock solution of 100 mg mL^{-1} Irgacure 2959 (Ciba Specialty Chemicals; Tarrytown, NY, USA) was prepared in 1-vinyl-2-pyrolidone and added to the hydrogel precursor solution at a 0.2% w/v photoinitiator concentration. The resulting solution polymerized within 5 min on exposure to UV light (365 nm, 17.5 mW cm^{-2}).

To demonstrate the utility of this device array in integrating non-photopolymerizable polymers, a temperature-polymerized collagen hydrogel was also polymerized in the compression chambers. Collagen gels were made from bovine type I collagen (Vitrogen Purified Collagen 100), obtained at 3.41 mg mL^{-1} in acetic acid. Equal parts of 10× concentrated DMEM, fetal bovine serum, penicillin–streptomycin, and 0.25 M sodium bicarbonate were prepared and mixed with 9% v/v 0.01 M sodium hydroxide to form a neutralization buffer. A 35% v/v solution of the neutralization buffer in type I collagen polymerized within 2 h at 37 °C.

2.4. Biomaterial integration

Both PEG and collagen polymers were integrated into the device by pipetting 250 μL of the liquid prepolymer onto

the hydrophobic PDMS device surface. In order to fill the 500 μm diameter compression chambers with the polymer, it was necessary to use a 25G needle under a dissecting microscope (SZX7; Olympus; Markham, ON, Canada) to remove the trapped air bubbles.

Once the array was filled, excess precursor solution was aspirated carefully from regions away from the compression chambers. A glass coverslip was then placed on top of the chambers. The hydrogels were polymerized by either placing the array beneath a Blakray UV illumination lamp (UVP; Ottawa, ON, Canada) for 5 min in the case of PEG, or in a 37 °C incubator for 2 h in the case of collagen. The glass coverslip was then carefully slid aside and replaced with a porous sintered metal disc (316L Stainless Steel, 5 μm grade; Chand Eisenmann Metallurgical; Burlington, ON, Canada) to allow biomaterial hydration and enable fluid movement during compression of the hydrogels (figure 2(*B*)). Following complete polymerization of the biomaterial, the device is actuated and the fully formed biomaterial undergoes compression.

2.5. Confocal imaging and analysis

To determine PEG hydrogel deformation, 1 μm diameter polystyrene fluorescent beads (Bangs Laboratories; Fisher, IN, USA) were added to the liquid prepolymer in a 1:1000 ratio. A confocal microscope (Fluoview 300, 10× ELWD objective; Olympus) was used to collect three-dimensional images of each hydrogel microconstruct when at rest and under compression. The image stacks were resliced vertically, for three separate cross sections of the microconstruct (figures 2(*D*) and (*E*)). Hydrogel deformation was independently assessed for each cross section and reported as a mean ± standard deviation of the total hydrogel deformation for each unit on the array.

2.6. Finite element simulations

Finite element simulations were performed using ABAQUS 6.6 (Dassault Systèmes Simulia Corp.; Providence, RI, USA) and ANSYS 9.0 (ANSYS Inc.; Canonsburg, PA, USA). A large deformation nonlinear hyperelastic finite element model was used to account for nonlinearities that arise from large deformation, contact sliding between the PEG hydrogel and the rigid plate, and material nonlinearity. An eight-node second-order axisymmetric element with displacement-pressure hybrid formulation was chosen to discretize the hydrogel and model the cylindrical microconstruct. The hydrogels were assumed to be isotropic and homogeneous and were described by a finite strain hyperelastic neo-Hookean constitutive model [27]. Based on the specific composition of PEG used in these studies, the initial shear modulus and bulk modulus were taken to be 40 and 53.2 kPa, respectively [28].

The interaction between the hydrogel and the loading piston was considered as a surface-based contact problem with the loading piston modelled as a rigid surface in contact with the deformable gel surface. Traction-free finite sliding was allowed between the gel base surface and the rigid plate. The mesh was refined near the edge of the rigid plate to account for the high strain gradient in this region. The element sizes in this region were between 1.54 and 2.05 μm in the radial direction and 5.07 μm through the thickness direction. In other regions of the model, the element sizes were approximately 12.25 μm in the radial direction and between 5.07 and 13.93 μm through the thickness direction.

The applied load was modelled as a prescribed displacement of the rigid plate. In simulations of unconfined compression, gel displacement was constrained at the top surface. To simulate confined compression, displacements were constrained at both the top and side surfaces. Semi-confined compression was simulated by constraining gel displacement at the top and side surfaces, with a rigid plate smaller than the gel diameter. In all cases, strain results in the axial, circumferential and radial directions are reported as mean ± standard deviation through the hydrogel thickness.

3. Results and Discussion

Three-dimensional deformation of cells in microdevices has been previously demonstrated through electrothermally deforming suspended cells [29] or by direct contact with a deflecting membrane [30, 31]. To take advantage of parallel operation of microfabricated systems for tissue engineering and to mimic more physiologically relevant cellular environments, it is necessary to study cells within an encapsulating matrix material. Our initial work established an array-based tool for unconfined compression of cell-laden biomaterials [23]. This work addresses issues of biomaterial versatility and strain heterogeneity in that system, by using a semi-confined compression scheme for hydrogel deformation.

3.1. Versatility in incorporating biomaterial types

Incorporating hydrogel microconstructs into our first-generation unconfined compression platform required photopolymerization and micropatterning of the biomaterial array. Photoinitiated free-radical polymerization of hydrogels is generally toxic to cells [32], and careful optimization is required to ensure complete polymerization while maintaining reasonable cell viability [23]. Hence, time-consuming optimization procedures are required for each selected biomaterial. Furthermore, this requirement limits the range of biomaterials compatible with the compression array.

The semi-confined compression system presented in this work addresses this issue by trapping the biomaterial prepolymer over the loading piston prior to polymerization. The versatility of this technology is demonstrated by incorporating collagen, a temperature-polymerized hydrogel into the compression chambers (figure 2(*C*)), in addition to the photopolymerized PEG material used in our previous and current studies.

The ability to incorporate various biomaterials regardless of polymerization mechanisms makes the semi-confined device platform more versatile in addressing problems in tissue engineering. In addition to the integrated influence of scaffold material and biochemical factors on cell function, the mechanical stiffness of the biomaterial itself can significantly

influence cell function [33]. Furthermore, there exists a complex relationship between the stiffness of the biomaterial, applied compression and cell deformation, as the surrounding matrix may shield the cell from strain [34]. Hence, the ability to use multiple biomaterials and multiple formulations of the same biomaterial in these devices will be of importance in identifying critical parameters in tissue engineering systems. Inclusion of multiple biomaterials on the same device may be possible with a microfluidic channel delivery system integrated into the compression chambers. Furthermore, the use of commercially available liquid handling systems in combination with microfabricated wells can enable systematic manipulation of mechanical, material and chemical microenvironmental parameters in three-dimensional culture.

3.2. Comparison with current technologies

In order to provide comparable simulations and measurements between strain profiles generated in the current device and in our previous work [23], the PEG biomaterial was selected for all finite element simulations and biomaterial-deformation studies. Similar analysis is applicable to studying other hyperelastic biomaterials.

Figure 3(*A*) demonstrates the strain field generated within a 3D PEG matrix under unconfined compression in our previous device array. To prevent loss of the photopolymerized hydrogel during handling of the device, it was necessary to bind the top of the hydrogel to the stationary wall, generating strain heterogeneity in the device. Radial, circumferential (hoop) and axial strains across the gel radius have similar mean values through the gel thickness. However, radial and circumferential strains range from 0.1% to 6.1% and axial strains range from 3.6% to 14.2% through the 200 μm thickness of the gel (figures 3(*A*)–(*C*) report this heterogeneity as standard deviations through the gel thickness). These non-uniformities cause a substantial strain gradient which may confound experimental analysis and interpretation of biological results.

A possible solution to the issue of strain uniformity is to use a confined compression system, in which a tightly fitted piston compresses a hydrogel within a closed environment (figure 3(*B*)). Confined compression is used in the FlexCell Compression System (FlexCell International Corporation; Hillsborough, NC, USA), a commercially available platform for macroscale mechanical compression of biomaterials [35]. Axial strains obtained through confined compression are highly uniform through the biomaterial, with no radial or circumferential strain, creating a well-defined mechanical environment. However, forming a confined compression platform on the microscale is challenging due to (1) stringent fabrication requirements for precisely aligned microstructures; and (2) unfavourable scaling laws, in which surface area-related stiction between the loading piston and the chamber walls greatly exceeds the volume-related restorative spring forces generated by vertical deflection of the piston. Once the piston touches the chamber wall, it requires a large restoring force to overcome stiction, which the thin, microfabricated actuation film underlying the piston cannot provide.

Semi-confined compression can be a suitable approach for microfabricated devices to increase throughput over conventional compression equipment, while avoiding the issues of strain heterogeneity in unconfined compression and technological difficulties in confined compression. Figure 3(*C*) demonstrates a typical strain profile in semi-confined compression, in which strains are relatively uniform in the central portion of the hydrogel but become heterogeneous towards the radial edges of the cylindrical hydrogel. The uniform strain in the central portion is suitable for microscopic analysis of these compressed biomaterials, as it is relatively simple to specify an area for analysis within a central cylindrical region of interest. Through the thickness of the hydrogel, strain varies by $\pm 1\%$ within a radius of 125 μm, or by $\pm 2.2\%$ within a 150 μm radius, substantial improvements over the unconfined compression system.

The relative size of the gap between the loading piston and the confining wall in comparison to the diameter of the hydrogel microconstruct is a critical parameter in determining the strain uniformity within the gel (figure 4). Decreases in gap size will present a loading condition approaching that of confined compression, hence improving strain uniformity in the bulk of the hydrogel. For these experiments, a 50 μm gap was used to ensure a high yield of successful devices. In order to increase the biomaterial volume undergoing uniform strain, an alternative to decrease the gap size would be to reduce experimental throughput and increase the microconstruct diameter, presenting a greater volume of uniform strain.

3.3. Strain characterization

Strains generated in the PEG biomaterial constructs across the semi-confined compression microdevice for an applied pressure of 55 kPa were characterized using a combination of confocal microscopy and finite element analysis. A pressure of 55 kPa was experimentally found to achieve the largest unimpeded displacement of the loading pistons into the compression chambers, thereby demonstrating the maximum strains achievable in a semi-confined compression device of these dimensions. Confocal microscopy was used to determine the global deformation of the cylindrical PEG microconstructs (figure 5). For brevity in presentation, the deformations measured with confocal imaging were assigned nominal strain values of 20%, 30%, 40% and 45% across the four different actuation cavity sizes in the microfabricated array, based on the calculated differences in hydrogel thickness before and after compression (values reported in figure 5). The non-linearity observed in nominal strains generated across the array is likely due to the loading piston approaching the maximum displacement for which the system was designed. This nonlinearity at the limits of piston displacement can be avoided by reducing the maximum strains produced, using actuation pressures less than 55 kPa. For these proof-of-concept experiments, device parameters were not optimized to generate uniformly increasing strains across the array. This can be achieved by developing analytical or computational models to relate applied pressure, actuation cavity dimensions,

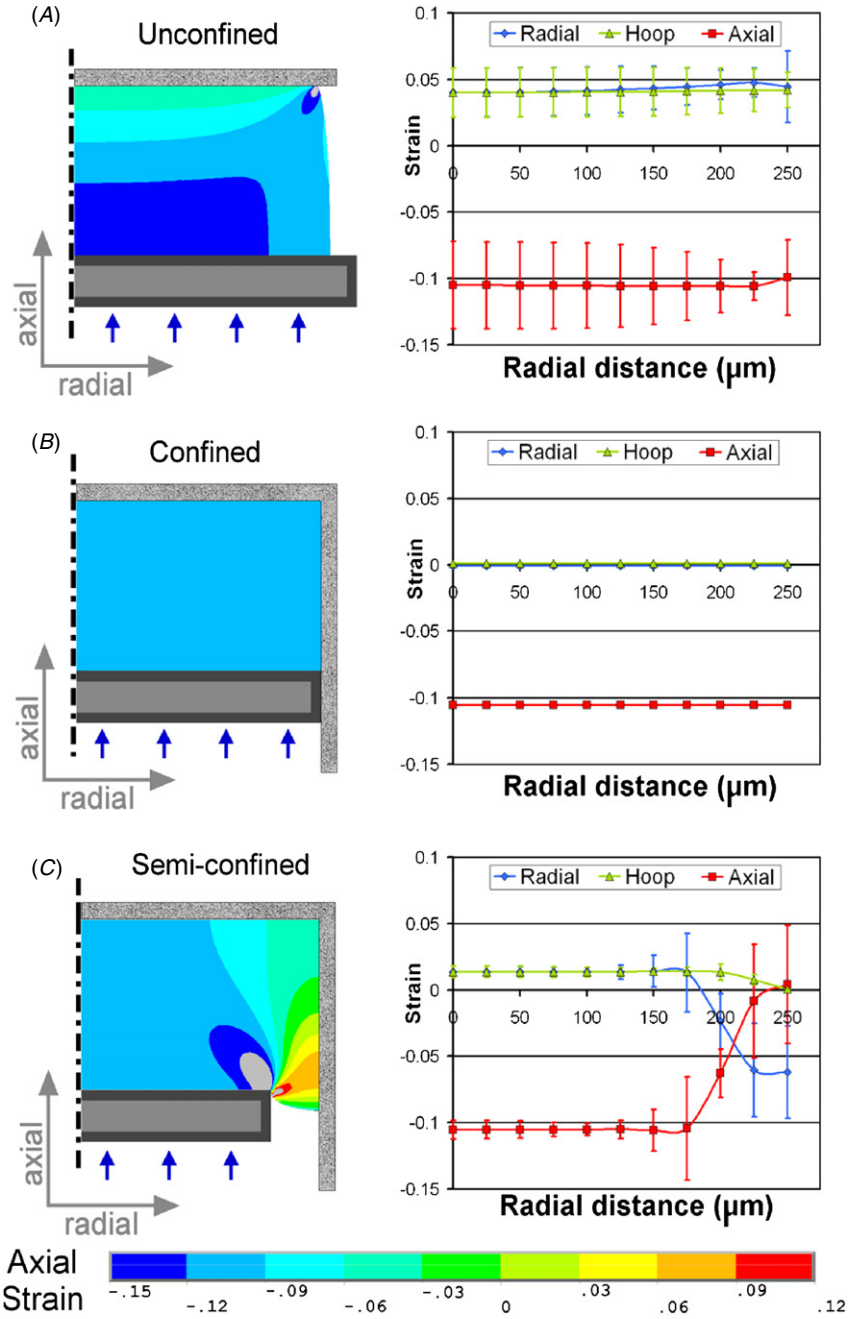

Figure 3. Comparison of simulated compression models. (*A*) Unconfined compression in our first generation compression platform generates a heterogeneous strain distribution within the hydrogel, but is relatively simple to produce in a microfabricated system. (*B*) Confined compression applies uniform strain to the biomaterial, but is challenging to microfabricate. (*C*) Semi-confined compression creates a central region of uniform strain distribution, and is possible to microfabricate using current techniques. All cylindrical axisymmetric strain fields are generated in identical material models for an applied compression of 10%. Plotted values for radial, circumferential, and axial strains represent the mean and standard deviation of strain values through the axial thickness of the hydrogel.

and material properties to loading piston displacement, and designing the devices to create conditions relevant to the specific biological system being studied.

To characterize local strains generated within the gel as a result of these applied deformations, finite element simulations were conducted at these nominal strain values (figure 6). Results demonstrate large axial strains similar in magnitude to the applied compression, and relatively uniform within a 250 to 300 μm diameter region of the 500 μm diameter cylindrical hydrogel. Radial and circumferential strain magnitudes were significantly smaller than compressive axial strains within this uniform region. Strains were generally of higher magnitudes than those generated in the previous unconfined compression array. While the unconfined compression system generated nominal strains ranging from 6% to 26% [23], the semi-confined platform generates nominal strains ranging from 20%

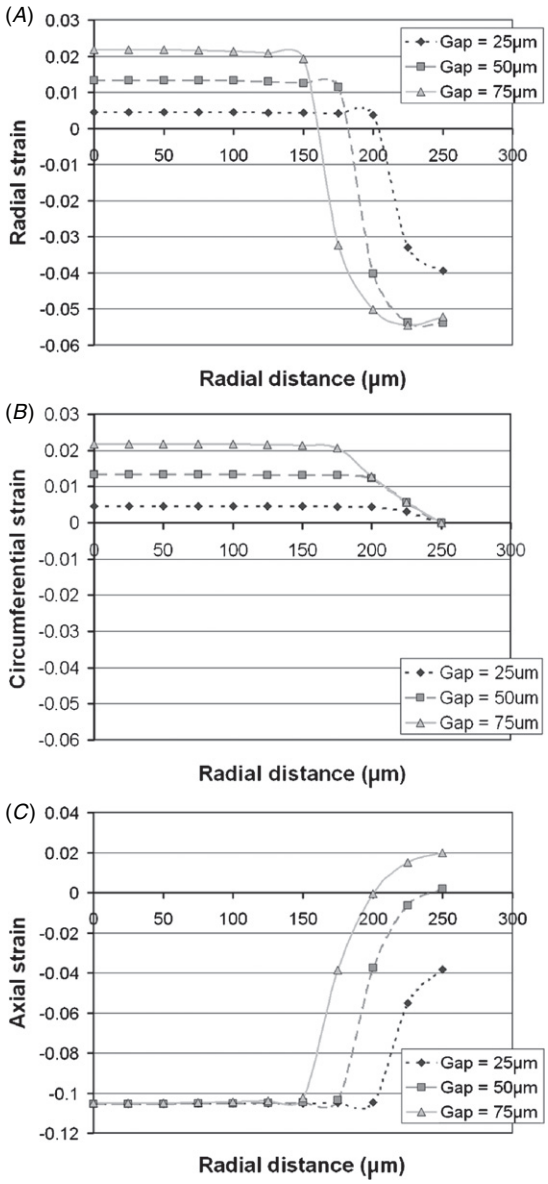

Figure 4. Simulated effect of a gap size between the loading piston and the compression chamber side wall on strain distribution within semi-confined cylindrical hydrogel constructs for (*A*) radial, (*B*) circumferential, and (*C*) axial strains. Error bars have been omitted for clarity, but follow similar patterns as in figure 3(*C*). Standard deviations reduce in magnitude with decreasing gap size in the central region of the hydrogel under uniform strain.

to 45%. This is due to differences in the thickness of the hydrogel microconstruct; similar compression stroke lengths in short and long materials generate significantly different strain magnitudes.

Although the finite element analyses presented here capture the nonlinear hyperelastic material properties of the deforming hydrogel [27], they do not account for other mechanical factors that may be of importance. Transient fluid pressures generated during deformation of the porous hydrogel may influence cell function [36]. In microfabricated hydrogels, the magnitude and duration of transient fluid flow is currently unknown, as scaling laws lead to a reduction in volume of the fluid reservoir, and a relative increase in

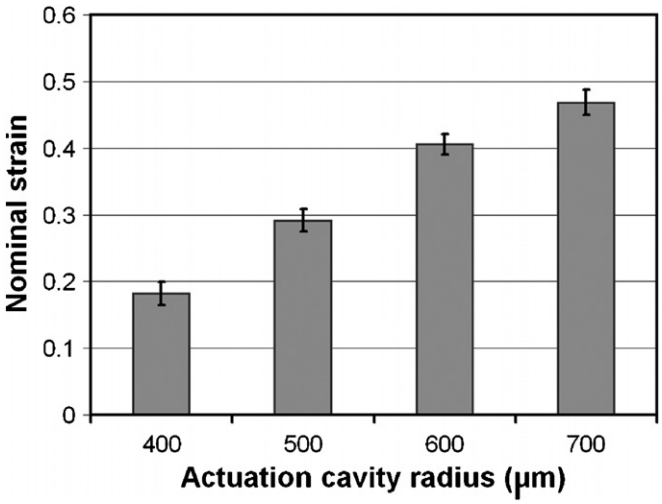

Figure 5. Experimental characterization of PEG hydrogel deformation for an applied pressure of 55 kPa across the microdevice array. Increasing actuation cavity size increases strains applied to the cylindrical microconstructs. Nominal strain values reported are for the deformation of the loading piston into the biomaterial, and error bars represent the standard deviation in measurement for a single microconstruct ($n = 3$).

the surface area through which fluid can exit. The use of a porous metal disc to constrain the gels should allow for rapid fluid drainage, and theoretically, rapid drainage of a small quantity of fluid should limit the transient hydrostatic pressures generated in the microconstructs. Further studies are needed to determine the importance of these transient fluid pressures on the microscale.

The mechanical strains demonstrated in these experiments are substantially higher than those necessary to replicate *in vivo* compressive loading conditions in mineralized tissue, such as bones and teeth. Instead, they may be more relevant to softer tissues typically studied under simple compressive loading such as cartilage [37] or intervertebral discs [38] or to tissues undergoing large local compressive deformations such as cardiac valve leaflets [39] or the matrix surrounding lung alveoli [40, 41]. This range of strains could also be used as a model to study the effects of drugs and chemical stimulation on diseased or injured tissue in which the matrix undergoes increased compressive strains. Although this study demonstrates relatively high strains in the device, tailoring the range of strains to the specific biomedical application can be accomplished by reducing the applied pneumatic pressure to the actuation cavities or by increasing the stiffness of the membrane supporting the loading piston (figure 1).

In this work we have demonstrated a 'semi-confined' compression approach as being well suited to establishing microfabricated mechanically dynamic cell culture platforms, demonstrating advantages in biomaterial versatility and strain uniformity. Further work is required before an array of these devices is validated for high-throughput screening studies. Specifically, issues of intra- and inter-device variabilities of applied strains must be characterized and addressed. As demonstrated in our previous works [13, 23, 25], similarly fabricated devices can be used to

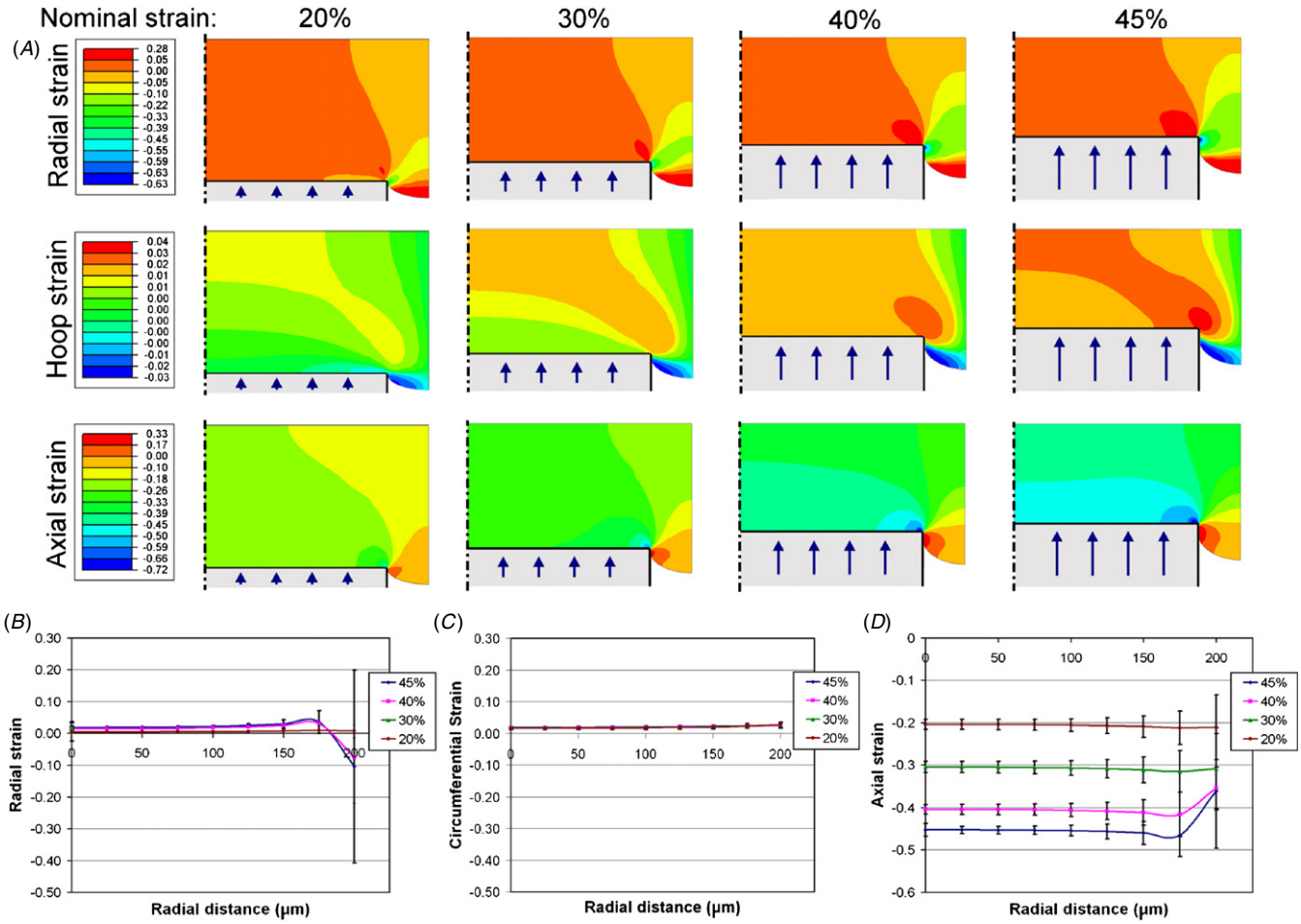

Figure 6. Simulation of local strains within hyperelastic PEG hydrogel constructs in the microfabricated device, based on experimental data. (*A*) Axisymmetric FEA images of radial and axial engineering strains demonstrate the central region of uniform strains which match closely to the applied nominal strains of 20%, 30%, 40% and 45%. (*B*)–(*D*) Mean and standard deviations of engineering strain for the (*B*) radial, (*C*) circumferential and (*D*) axial strains obtained through the axial thickness of the deforming hydrogel.

generate relatively uniform mechanical conditions in an arrayed format. It should be noted that in order to achieve such consistency between arrayed units of similar sizes, fabrication procedures required careful optimization to ensure uniform thickness across the microfabricated SU-8 master. Such optimization and characterization procedures remain to be performed for the semi-confined compression screening platform in this preliminary work, and are critical steps in establishing validated high-throughput screening tools for specific biological applications.

4. Conclusion

In order to enable parallel screen of mechanically active cell cultures, a MEMS-compatible actuation scheme was developed to apply a range of compressive loading conditions to biomaterial microconstructs. The new 'semi-confined' compression device generates uniform compressive strains within a defined region of each cylindrical hydrogel, enabling the systematic evaluation of cellular response to precisely applied strains in a three-dimensional matrix. Characterization of deformation in the semi-confined biomaterial array demonstrates strains ranging from 20% to 45%. The system is also compatible with a range of polymerizable biomaterials, improving the applicability and versatility of the platform in conducting various studies. More broadly, when combined with other robotic and microfabricated technologies, the MEMS-based platform provides a feasible design for systematically manipulating biomaterial, mechanical and chemical factors in a three-dimensional environment, an approach which may be of importance in simulating physiological conditions for drug discovery, regenerative medicine, and tissue engineering.

Acknowledgments

The authors gratefully thank Professor Christopher Yip and Gary Mo from the Centre for Studies in Molecular Imaging for helpful advice, discussion and use of confocal microscopy equipment. They acknowledge microfabrication support from the Emerging Communications Technology Institute and the Toronto Microfluidics Foundry. They also acknowledge

financial support from the National Sciences and Engineering Research Council of Canada and the Canadian Institutes of Health Research (CHRPJ 323533-06); the Ontario Graduate Scholarship program to CM; the Heart and Stroke Foundation of Canada to RZ; and the Canada Research Chairs in Mechanobiology to CAS, and in Micro and Nano Engineering Systems to YS.

References

[1] Wang J H and Thampatty B P 2006 An introductory review of cell mechanobiology *Biomech. Model. Mechanobiol.* **5** 1–16

[2] Bonassar L J, Grodzinsky A J, Frank E H, Davila S G, Bhaktav N R and Trippel S B 2001 The effect of dynamic compression on the response of articular cartilage to insulin-like growth factor-I *J. Orthop. Res.* **19** 11–7

[3] McBeath R, Pirone D M, Nelson C M, Bhadriraju K and Chen C S 2004 Cell shape, cytoskeletal tension, and RhoA regulate stem cell lineage commitment *Dev. Cell* **6** 483–95

[4] Rehfeldt F, Engler A J, Eckhardt A, Ahmed F and Discher D E 2007 Cell responses to the mechanochemical microenvironment—implications for regenerative medicine and drug delivery *Adv. Drug. Deliv. Rev.* **59** 1329–39

[5] Martin I, Wendt D and Heberer M 2004 The role of bioreactors in tissue engineering *Trends Biotechnol.* **22** 80–6

[6] Bilodeau K and Mantovani D 2006 Bioreactors for tissue engineering: Focus on mechanical constraints: a comparative review *Tissue Eng.* **12** 2367–83

[7] Berry J L, Steen J A, Koudy Williams J, Jordan J E, Atala A and Yoo J J 2010 Bioreactors for development of tissue engineered heart valves *Ann. Biomed. Eng.* **38** 3272–9

[8] Altman G H, Lu H H, Horan R L, Calabro T, Ryder D, Kaplan D L, Stark P, Martin I, Richmond J C and Vunjak-Novakovic G 2002 Advanced bioreactor with controlled application of multi-dimensional strain for tissue engineering *J. Biomech. Eng.* **124** 742–9

[9] Kong H J, Liu J, Riddle K, Matsumoto T, Leach K and Mooney D J 2005 Non-viral gene delivery regulated by stiffness of cell adhesion substrates *Nat. Mater.* **4** 460–4

[10] Lee W C, Maul T M, Vorp D A, Rubin J P and Marra K G 2007 Effects of uniaxial cyclic strain on adipose-derived stem cell morphology, proliferation, and differentiation *Biomech. Model. Mechanobiol.* **6** 265–73

[11] MacKenna D A, Dolfi F, Vuori K and Ruoslahti E 1998 Extracellular signal-regulated kinase and c-Jun NH2-terminal kinase activation by mechanical stretch is integrin-dependent and matrix-specific in rat cardiac fibroblasts *J. Clin. Invest.* **101** 301–10

[12] Zandstra P W 2004 The opportunity of stem cell bioengineering *Biotechnol. Bioeng.* **88** 263

[13] Moraes C, Chen J H, Sun Y and Simmons C A 2010 Microfabricated arrays for high-throughput screening of cellular response to cyclic substrate deformation *Lab Chip* **10** 227–34

[14] Young E W K, Wheeler A R and Simmons C A 2007 Matrix-dependent adhesion of vascular and valvular endothelial cells in microfluidic channels *Lab Chip* **7** 1759–66

[15] Kamotani Y, Bersano-Begey T, Kato N, Tung Y C, Huh D, Song J W and Takayama S 2008 Individually programmable cell stretching microwell arrays actuated by a Braille display *Biomaterials* **29** 2646–55

[16] Tan W, Scott D, Belchenko D, Qi H J and Xiao L 2008 Development and evaluation of microdevices for studying anisotropic biaxial cyclic stretch on cells *Biomed. Microdevices* **10** 869–82

[17] Gomez-Sjoberg R, Leyrat A A, Pirone D M, Chen C S and Quake S R 2007 Versatile, fully automated, microfluidic cell culture system *Anal. Chem.* **79** 8557–63

[18] Song J W, Gu W, Futai N, Warner K A, Nor J E and Takayama S 2005 Computer-controlled microcirculatory support system for endothelial cell culture and shearing *Anal. Chem.* **77** 3993–9

[19] Cukierman E, Pankov R, Stevens D R and Yamada K M 2001 Taking cell-matrix adhesions to the third dimension *Science* **294** 1708–12

[20] Buschmann M D, Gluzband Y A, Grodzinsky A J and Hunziker E B 1995 Mechanical compression modulates matrix biosynthesis in chondrocyte agarose culture *J. Cell Sci.* **108** 1497–508

[21] Yanagisawa M, Suzuki N, Mitsui N, Koyama Y, Otsuka K and Shimizu N 2007 Effects of compressive force on the differentiation of pluripotent mesenchymal cells *Life Sci.* **81** 405–12

[22] Pelaez D, Huang C Y C and Cheung H S 2009 Cyclic compression maintains viability and induces chondrogenesis of human mesenchymal stem cells in fibrin gel scaffolds *Stem Cells Dev.* **18** 93–102

[23] Moraes C, Wang G, Sun Y and Simmons C A 2010 A microfabricated platform for high-throughput unconfined compression of micropatterned biomaterial arrays *Biomaterials* **31** 577–84

[24] Tabata Y 2009 Biomaterial technology for tissue engineering applications *J. R. Soc. Interface* **6** S311–24

[25] Moraes C, Sun Y and Simmons C A 2009 Solving the shrinkage-induced PDMS alignment registration issue in multilayer soft lithography *J. Micromech. Microeng.* **19** 065015

[26] Jo B H, Van Lerberghe L M, Motsegood K M and Beebe D J 2000 Three-dimensional micro-channel fabrication in polydimethylsiloxane (PDMS) elastomer *J. Microelectromech. Syst.* **9** 76–81

[27] Kloxin A M, Kloxin C J, Bowman C N and Anseth K S 2010 Mechanical properties of cellularly responsive hydrogels and their experimental determination *Adv. Mater.* **22** 3484–94

[28] Peyton S R, Raub C B, Keschrumrus V P and Putnam A J 2006 The use of poly(ethylene glycol) hydrogels to investigate the impact of ECM chemistry and mechanics on smooth muscle cells *Biomaterials* **27** 4881–93

[29] Zhang W Y, Gnerlich M, Paly J J, Sun Y H, Jing G S, Voloshin A and Tatic-Lucic S 2008 A polymer V-shaped electrothermal actuator array for biological applications *J. Micromech. Microeng.* **18** 075020

[30] Kim Y C, Kang J H, Park S J, Yoon E S and Park J K 2007 Microfluidic biomechanical device for compressive cell stimulation and lysis *Sensors Actuators* B **128** 108–16

[31] Kim Y C, Park S J and Park J K 2008 Biomechanical analysis of cancerous and normal cells based on bulge generation in a microfluidic device *Analyst* **133** 1432–9

[32] Liu V A and Bhatia S N 2002 Three-dimensional photopatterning of hydrogels containing living cells *Biomed. Microdevices* **4** 257–66

[33] Engler A J, Sen S, Sweeney H L and Discher D E 2006 Matrix elasticity directs stem cell lineage specification *Cell* **126** 677–89

[34] Guilak F and Mow V C 2000 The mechanical environment of the chondrocyte: a biphasic finite element model of cell–matrix interactions in articular cartilage *J. Biomech.* **33** 1663–73

[35] Brown T D 2000 Techniques for mechanical stimulation of cells *in vitro*: a review *J. Biomech.* **33** 3–14

[36] Mauck R L, Soltz M A, Wang C C, Wong D D, Chao P H, Valhmu W B, Hung C T and Ateshian G A 2000 Functional tissue engineering of articular cartilage through dynamic loading of chondrocyte-seeded agarose gels *J. Biomech. Eng.* **122** 252–60

[37] Carter D R and Wong M 2003 Modelling cartilage mechanobiology *Phil. Trans. R. Soc.* B **358** 1461–71

[38] Setton L A and Chen J 2004 Cell mechanics and mechanobiology in the intervertebral disc *Spine* **29** 2710–23

[39] De Hart J, Peters G W, Schreurs P J and Baaijens F P 2003 A three-dimensional computational analysis of fluid-structure interaction in the aortic valve *J. Biomech.* **36** 103–12

[40] Dale P J, Matthews F L and Schroter R C 1980 Finite element analysis of lung alveolus *J. Biomech.* **13** 865–73

[41] Gefen A, Elad D and Shiner R J 1999 Analysis of stress distribution in the alveolar septa of normal and simulated emphysematic lungs *J. Biomech.* **32** 891–7